

# 256 QAM Digital Coherent Optical Transmission Using Raman Amplifiers

Masato YOSHIDA<sup>†a)</sup>, Member, Seiji OKAMOTO<sup>†</sup>, Tatsunori OMIYA<sup>†</sup>, Student Members, Keisuke KASAI<sup>†</sup>, Member, and Masataka NAKAZAWA<sup>†</sup>, Fellow

**SUMMARY** To meet the increasing demand to expand wavelength division multiplexing (WDM) transmission capacity, ultrahigh spectral density coherent optical transmission employing multi-level modulation formats has attracted a lot of attention. In particular, ultrahigh multi-level quadrature amplitude modulation (QAM) has an enormous advantage as regards expanding the spectral efficiency to 10 bit/s/Hz and even approaching the Shannon limit. We describe fundamental technologies for ultrahigh spectral density coherent QAM transmission and present experimental results on polarization-multiplexed 256 QAM coherent optical transmission using heterodyne and homodyne detection with a frequency-stabilized laser and an optical phase-locked loop technique. In this experiment, Raman amplifiers are newly adopted to decrease the signal power, which can reduce the fiber nonlinearity. As a result, the power penalty was reduced from 5.3 to 2.0 dB. A 64 Gbit/s data signal is successfully transmitted over 160 km with an optical bandwidth of 5.4 GHz.

**key words:** coherent transmission, quadrature amplitude modulation, spectral efficiency, frequency-stabilized laser, optical phase-locked loop

## 1. Introduction

Transmission with high spectral efficiency employing multi-level modulation formats has attracted a lot of attention with a view to expanding the capacity of wavelength division multiplexing (WDM) transmission systems, because multi-bit information can be transmitted by one symbol data. Multi-level modulation also enables us to realize a high-speed system with low-speed devices, and therefore helps to enhance tolerance to chromatic dispersion and polarization mode dispersion as well as to reduce power consumption.

Recently, a number of experimental results have been reported in which multi-level phase-shift keying (PSK) or a combination of PSK and amplitude-shift keying (ASK) has been employed for such a purpose [1], [2]. Of these approaches, coherent quadrature amplitude modulation (QAM) [3]–[15] is one of the most spectrally efficient modulation formats. A  $2^N$  QAM signal processes  $N$  bits in a single channel, so it has  $N$  times the spectral efficiency of on-off keying (OOK). For example, if we can employ 256–1024 QAM, which was originally developed for microwaves, we may obtain enormous advantages such as an ultrahigh spectral efficiency exceeding 10 bit/s/Hz.

Orthogonal frequency division multiplexing (OFDM) is another approach that has attracted a lot of attention in

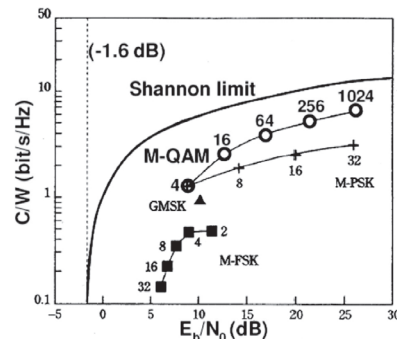


**Fig. 1** Spectral efficiency of M-ary QAM signal and the Shannon limit.  $E_b/N_0$  at BER =  $10^{-4}$  is shown assuming synchronous detection.

relation to transmission with high spectral efficiency. In OFDM transmission, the multi-carrier transmission of low-speed orthogonal subcarriers enables us to improve both spectral efficiency and dispersion tolerance by adopting high-level subcarrier modulation format and employing coherent detection [16]–[21].

The spectral efficiency of an M-ary QAM signal is shown in Fig. 1 as a function of the energy to noise power density ratio per bit,  $E_b/N_0$ . Here, ultimate spectral efficiency is given by the Shannon limit:

$$\frac{C}{W} = \log_2 \left( 1 + \frac{E_b}{N_0} \frac{C}{W} \right) \quad (1)$$

Here  $C$  and  $W$  are the channel capacity and signal bandwidth, respectively. Equation (1) is known the Shannon-Hartley theorem [22]. This figure indicates that, as the multiplicity  $M$  increases, the spectral efficiency of M-QAM approaches closer to the Shannon limit than other advanced modulation formats such as M-PSK or M-frequency-shift keying (FSK). The increase in  $M$ , however, requires a larger  $E_b/N_0$  value under the same BER. So the forward error correction (FEC) technique [23], which has been developed to realize a better BER performance with a lower  $E_b/N_0$ , plays an important role for realizing ultrahigh spectral efficiency by using ultra-multi-level QAM format.

Figure 2 shows recent transmission experiments with high spectral efficiency using polarization-multiplexed M-PSK [1], M-QAM [8]–[14], and OFDM [19]–[21] formats in which BER lower than the FEC limit of  $2 \times 10^{-3}$  was achieved. This figure indicates that the multiplicity of the QAM signals larger than 128 levels is needed to achieve a

Manuscript received June 30, 2010.

Manuscript revised November 16, 2010.

<sup>†</sup>The authors are with the Research Institute of Electrical Communication, Tohoku University, Sendai-shi, 980-8577 Japan.

a) E-mail: masato@iec.tohoku.ac.jp

DOI: 10.1587/transcom.E94.B.417

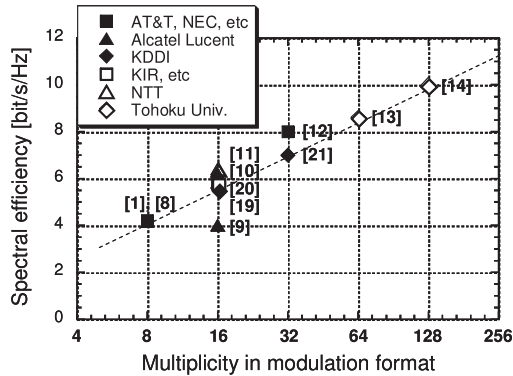


Fig. 2 Recent transmission experiments with high spectral efficiency.

spectral efficiency higher than 10 bit/s/Hz.

We have demonstrated a polarization-multiplexed 256 QAM coherent optical transmission over 160 km using homodyne detection with a frequency-stabilized laser and an optical phase-locked loop (OPLL) technique [15]. We adopted erbium-doped fiber amplifiers (EDFAs) as optical repeaters. However, there was a power penalty of as large as 5.3 dB at a BER of  $2 \times 10^{-3}$ . In this paper, we present an improved experimental result for a 256 QAM coherent optical transmission with Raman amplifiers and EDFAs. By reducing a launch power into the optical transmission line without optical signal-to-noise ratio (OSNR) degradation by using Raman amplifiers, fiber nonlinearity such as cross phase modulation (XPM) between the two polarizations, is suppressed, resulting in a power penalty reduction from 5.3 to 2.0 dB.

## 2. Fundamental Configuration and Key Components of QAM Coherent Optical Transmission

The fundamental configuration of a QAM coherent optical transmission is shown in Fig. 3. A CW,  $C_2H_2$  frequency-stabilized fiber laser is employed as a coherent light source [24]. The optical QAM signal can be easily generated with an IQ modulator [25] consisting of two nested Mach-Zehnder (MZ) modulators and a 90-degree phase shifter driven by QAM signals from arbitrary waveform generator (AWG). A transmitted QAM signal and a local oscillator (LO) signal are heterodyne detected with a photo detector (PD). Then, the optical QAM signal is converted to an intermediate frequency (IF) signal. Here, an OPLL technique [26] using a high-speed free-running laser as an LO is also very important as regards the automatic frequency control of the IF carrier. The IF signal is then A/D converted and accumulated in a digital signal processor (DSP). All digital signals are demodulated into I and Q data and finally into a binary sequence in the DSP. Because of the software demodulation, this transmission system operates in an off-line condition. In this section, we describe these key components for QAM coherent transmission.

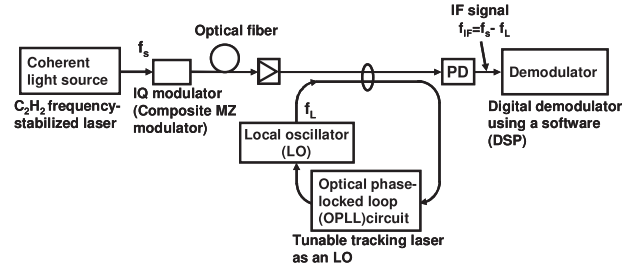


Fig. 3 Fundamental configuration for QAM coherent optical transmission system.

### 2.1 $C_2H_2$ Frequency-Stabilized Erbium-Doped Fiber Ring Laser

A stable optical frequency in the  $1.5 \mu\text{m}$  region is indispensable as a light source for QAM coherent transmission.  $C_2H_2$  molecules have been utilized as a frequency standard to stabilize the frequency of semiconductor and fiber lasers at  $1.55 \mu\text{m}$  [27]. We constructed a  $C_2H_2$  frequency-stabilized, polarization-maintaining erbium-doped fiber ring laser [24] and used it as a transmitter. A  $1.5 \text{ GHz}$  ultranarrow polarization-maintaining fiber Bragg grating (FBG) filter [28] was installed in a 4 m-long laser cavity to realize single-frequency operation. The laser output power was 4.5 mW with a pump power of 200 mW. The linewidth measured by using a delayed self-heterodyne detection method [29] with a 50 km delay fiber was 4 kHz. The frequency stability evaluated from the square root of the Allan variance [30] was  $2.5 \times 10^{-11}$  for an integration time,  $\tau$ , of 1 s, and  $6.3 \times 10^{-12}$  for a  $\tau$  of 100 s. Excellent short and long-term stabilities were obtained.

### 2.2 Optical PLL for Coherent Transmission Using Heterodyne Detection with Fiber Lasers

The precise optical phase control of light sources is very important for coherent optical transmission with heterodyne detection. The optical frequency difference between a transmitter and an LO must be kept constant in order to obtain a stable IF signal. In a heterodyne detection system, the use of a high-speed OPLL is a key technique for automatic frequency control. The linewidth of the IF signal is evaluated as

$$\sigma_{\phi}^2 = \frac{\delta f_S + \delta f_L}{2f_c} \quad (2)$$

where  $\delta f_S$  and  $\delta f_L$  are the linewidth of the transmitter and LO, and  $f_c$  is the bandwidth of the feedback circuit [31]. This indicates that the reduction of the phase noise (linewidth) of the two lasers and the large bandwidth of the feedback circuit are very important factors as regards realizing a precise OPLL. Of the many available lasers, the fiber laser is suitable for an OPLL because of its low phase noise (narrow linewidth), because this allows the laser to be applied directly to an OPLL system.

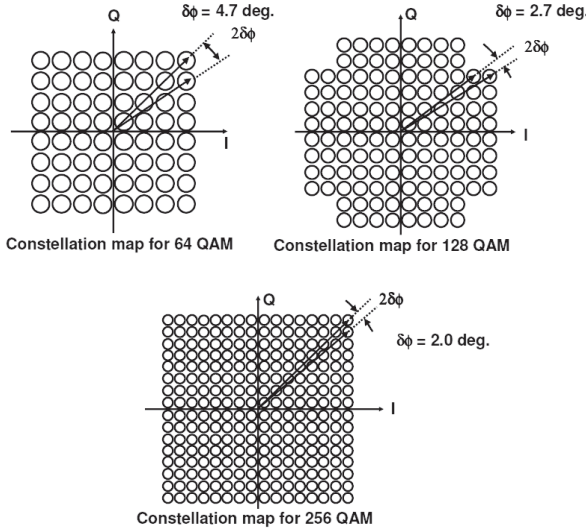


**Fig. 4** Constellation maps of 64, 128, and 256 QAM signals and the comparison of the tolerable phase noise.

In our OPLL circuit, we used a frequency-tunable erbium-doped fiber laser as an LO with a linewidth of 4 kHz. The bandwidth of the feedback circuit consisting of loop filters was 1 MHz. The phase noise variance (RMS) of the IF signal under OPLL operation was as low as 0.3 degrees. This low phase noise of the IF signal in spite of the relatively large PLL bandwidth is attributed to the narrow linewidth of the fiber laser.

The tolerance of the phase noise for 64, 128, and 256 QAM signals can be estimated from constellation maps. As shown in Fig. 4, the half angle between the two closest symbols is  $\delta\phi = 4.7, 2.7,$  and  $2.0$  degree for 64, 128, and 256 QAM, respectively, which correspond to the tolerable phase noise. Therefore, the RMS phase noise of 0.3 degree is sufficiently small for demodulating even a 256 QAM signal.

### 2.3 IQ modulator

An optical IQ modulator is composed of three MZ interferometers based on LN waveguide [25]. In the LN-based IQ modulator, surface acoustic wave are generated by the piezoelectric effect in the LN crystal, which degrades the low-frequency response of the modulator [32]. To suppress the acoustic wave, we tapered the edge of the modulator and reduced its thickness. Figures 5(a) and (b) show the E/O characteristics of IQ modulators with the conventional and new structures, respectively. The low-frequency response was successfully improved with the new structure. This improvement plays a very important role in increasing the multiplicity level in QAM transmission.

### 2.4 Digital Demodulator

Figure 6 shows a schematic diagram of our digital demodulator. The IF signal data are first A/D converted and accumulated in a high-speed digital scope, whose sampling

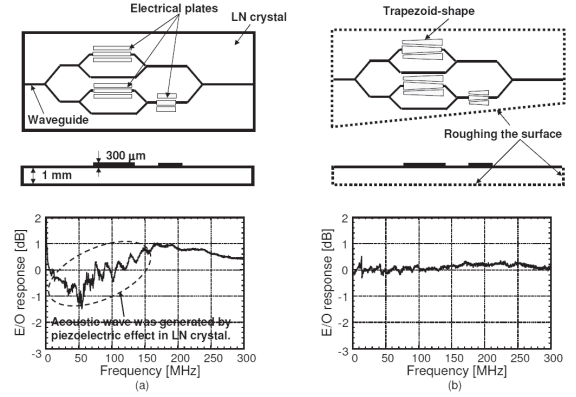


**Fig. 5** Improvement of IQ modulator. Schematic diagram of the modulator and its E/O characteristics of IQ modulator (a) before and (b) after improvement.

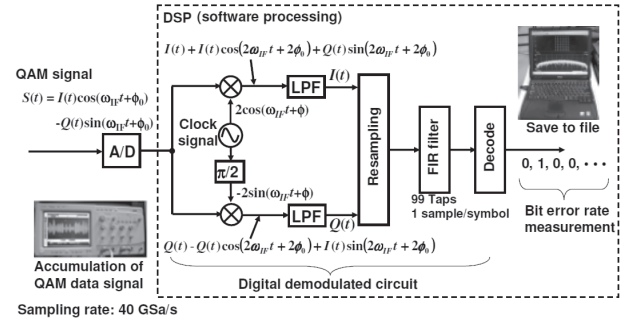


**Fig. 6** Diagram of digital signal processor.

frequency, bandwidth, and vertical resolution are 40 Gsample/s, 12 GHz, and 8 bit, respectively. Then I and Q data are demodulated with software by multiplying synchronous cosine and sine functions, respectively, onto I+Q data. Finally the demodulated data are converted into binary data in the software decoder. Here the center frequency of the IF signal is determined by an operation frequency of the synthesizer used in the OPLL circuit. In this off-line system, we send the frequency information to the DSP, and the clock signal used for the IQ demodulation is recovered by the software processing.

## 3. 256 QAM Coherent Optical Transmission

We undertook a single-channel 256 QAM transmission over 160 km based on the configuration described above. By introducing polarization multi-plexing in a 4 Gsymbol/s 256 ( $2^8$ ) QAM transmission, a data speed of 64 Gbit/s was obtained. In our previous work, the launch power into the optical transmission line was set at  $-2$  dBm [15]. This power level was chosen to optimize the nonlinearity and OSNR. This time, we adopted Raman amplifiers and reduced the launch power to  $-8$  dBm with the same OSNR as our previous work. As a result, the nonlinear effect in the optical transmission line was suppressed and the BER performance was successfully improved.

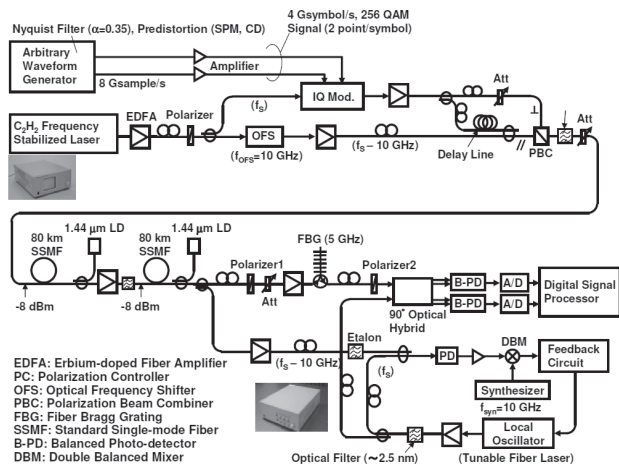


Fig. 7 Experimental setup for Pol-Mux, 4 Gsymbol/s, 256 QAM coherent optical transmission over 160 km using Raman amplifiers.

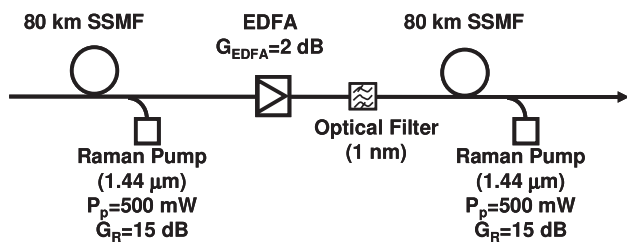


Fig. 8 Configuration of 160 km transmission fiber link.

### 3.1 Polarization-Multiplexed 4 Gsymbol/s, 256 QAM Transmission Setup

The experimental setup is shown Fig. 7. The frequency-stabilized laser output ( $f_s$ ) is split into two arms via an erbium-doped fiber amplifier (EDFA). One arm is coupled to an IQ modulator, where the beam is modulated with a 4 Gsymbol/s, 256 QAM baseband signal generated by an AWG running at 8 Gsample/s. Here, standard electrical amplifiers for data modulation with a bandwidth of more than 10 GHz are used to amplify the baseband signal. We employed a raised-cosine Nyquist filter [33] with a roll-off factor of 0.35 at the AWG using a software program to reduce the bandwidth of the QAM signal to 5.4 GHz. A signal with a carrier frequency is then orthogonally polarization-multiplexed with a polarization beam combiner (PBC). The other frequency-stabilized beam is coupled to an optical frequency-shifter (OFS), which provides a frequency downshift of 10 GHz ( $f_s - 10$  GHz) against the data signal. Then, the frequency-shifted signal is used as a pilot tone signal that tracks the optical phase of the LO under optical PLL operation.

The polarization of the pilot tone signal is the same as one of the polarization axes of the two QAM signals. These signals are combined and launched into a 160 km transmission fiber link, which is composed of two 80 km SSMF, two backward Raman amplifiers and an EDFA, as shown in

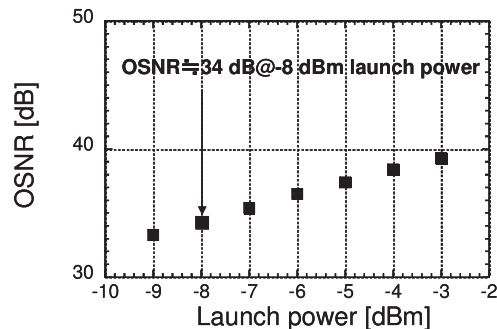


Fig. 9 OSNR versus launch power.

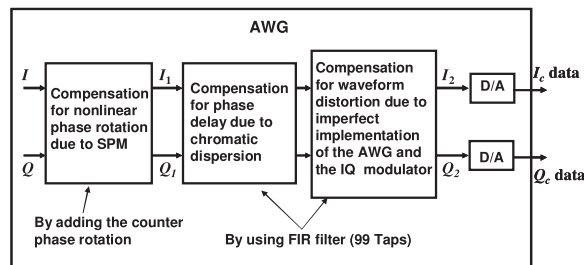


Fig. 10 Block diagram of compensation for waveform distortion.

Fig. 8. The pump power and gain of the Raman amplifiers were 500 mW and 15 dB, respectively. Figure 9 shows the OSNR after a 160 km transmission versus the launch power. With a launch power of  $-8$  dBm, the OSNR was 34.3 dB. This OSNR is almost the same as that obtained in our previous work, which we undertook without a Raman amplifier. We set the launch power at  $-8$  dBm and compared the BER performance in experimental results obtained with and without a Raman amplifier to discuss the nonlinear effect in the optical transmission line.

At the receiver, the QAM signals are polarization-demultiplexed with Polarizer1. Here, we define the power launched into an EDFA preamplifier as the received power. The amplified signal then passes through an FBG optical filter with a 5 GHz bandwidth and Polarizer2 for ASE noise reduction. After that, the signal is homodyne-detected with a 90-degree optical hybrid using an LO signal from a frequency tunable fiber laser whose phase is locked to the transmitted pilot tone signal. After detection with balanced photodiodes (B-PDs), the data are A/D-converted and post-processed with a DSP in an off-line condition.

### 3.2 Compensation for Waveform Distortion

Waveform distortions of the QAM signal are caused by imperfect implementation of hardware, for example the AWG and the IQ modulator, and chromatic dispersion and nonlinear effect in the optical fiber transmission line. We introduced pre-distortion for the waveform compensation into QAM signal using software at the AWG. Figure 10 shows the block diagram of the compensation for the waveform distortion. Self-phase modulation (SPM) can be compen-

sated by introducing an artificial phase rotation that cancels the SPM-induced phase rotation [34]. The SPM-induced phase rotation is given by

$$\Delta\phi_c = \gamma PL_{eff} \times N, \quad (3)$$

$$L_{eff} = \frac{1}{\alpha} (1 - e^{-\alpha L}) \quad (4)$$

where  $\gamma$  is a nonlinear coefficient,  $P$  is the transmission power,  $L$  is the span length,  $L_{eff}$  is the effective span length that takes account of the fiber loss  $\alpha$  defined as Eq. (4), and  $N$  is the number of spans. From the parameters corresponding to the present experiment,  $\gamma = 1.5 \text{ W}^{-1}\text{km}^{-1}$ ,  $\alpha = 0.2 \text{ dB/km}$  ( $0.046 \text{ km}^{-1}$ ),  $L = 80 \text{ km}$ , and  $N = 2$ , we obtain  $k = \Delta\phi/P = 0.064 \text{ rad/mW}$ . We introduced SPM compensation by adding a phase shift

$$\Delta\phi_c = -k \{P_I(t) + P_Q(t)\} \quad (5)$$

to the QAM signal, where  $P_I$  and  $P_Q$  are the optical powers of the  $I$  and  $Q$  data, respectively. The SPM compensated QAM data ( $I_1$ ,  $Q_1$ ) is given by

$$\begin{pmatrix} I_1(t) \\ Q_1(t) \end{pmatrix} = \begin{pmatrix} \cos(\Delta\phi_c(t)) & -\sin(\Delta\phi_c(t)) \\ \sin(\Delta\phi_c(t)) & \cos(\Delta\phi_c(t)) \end{pmatrix} \begin{pmatrix} I(t) \\ Q(t) \end{pmatrix} \quad (6)$$

Other waveform distortions caused by chromatic dispersion and imperfect implementation of hardware were compensated by using a finite impulse response (FIR) filter [35] with 99 taps. The second compensated QAM data ( $I_2$ ,  $Q_2$ ) is given by

$$\begin{pmatrix} I_2(t) \\ Q_2(t) \end{pmatrix} = \sum_{n=-49}^{49} \begin{pmatrix} \text{Re}(h(nT)) & -\text{Im}(h(nT)) \\ \text{Im}(h(nT)) & \text{Re}(h(nT)) \end{pmatrix} \begin{pmatrix} I_1(t-nT) \\ Q_1(t-nT) \end{pmatrix} \quad (7)$$

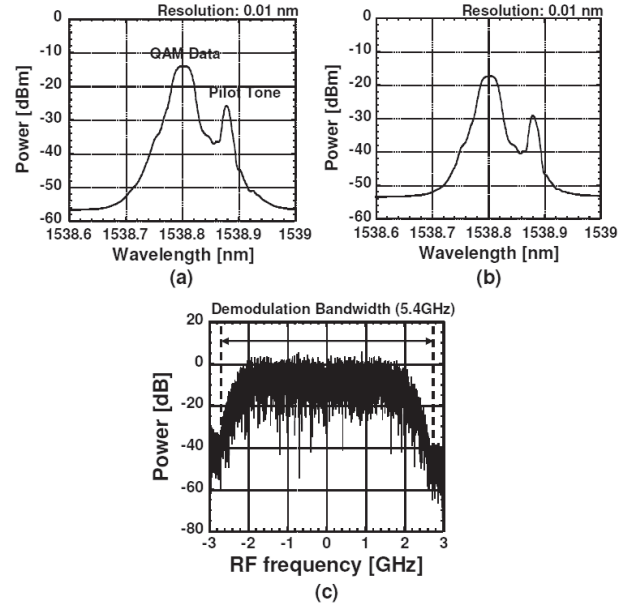
where  $h(nT)$  is the impulse response of the QAM coherent transmission system, and  $T$  is symbol period. Finally, the compensated QAM analog data signals ( $I_c$ ,  $Q_c$ ) are output via D/A converters.

In addition, we employed an adaptive FIR filter in the DSP at the receiver as shown in Fig. 6 to compensate for the waveform distortion caused by the fluctuation in the optical transmission line.

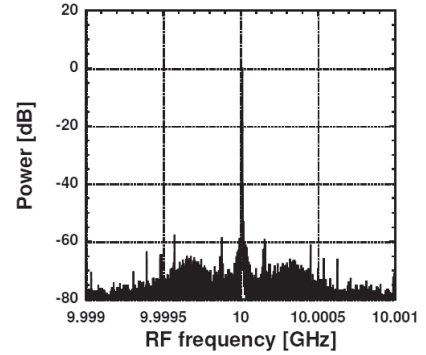
### 3.3 Transmission Results

Figure 11 shows the optical spectra of the QAM signal before and after 160 km transmission, (a) and (b) respectively, and the electrical spectrum of the demodulated signal at the DSP (c). Here the launch power of the QAM data signal and tone signal were  $-8$  and  $-24$  dBm, respectively. The OSNR was reduced by 6.5 dB due to ASE noise. The demodulation bandwidth was set at 5.4 GHz due to the adoption of a Nyquist filter.

Figure 12 shows the electrical spectrum of a beat signal between the pilot tone ( $f_s - 10$  GHz) and LO signals ( $f_L = f_s$ ) under optical PLL operation after 160 km transmission. The beat frequency was set at 10 GHz to realize homodyne detection, that is, the carrier frequency of the QAM signal



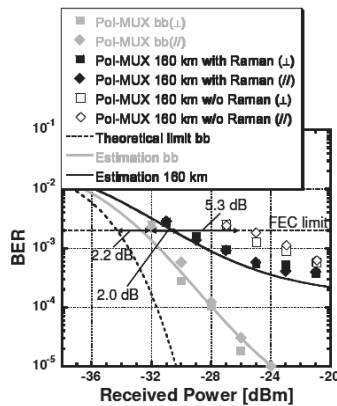
**Fig. 11** Optical spectra of the QAM signal before (a) and after (b) 160 km transmission, and (c) electrical spectrum of the demodulated signal at the DSP.



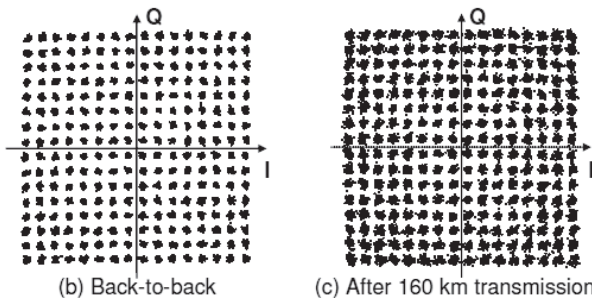
**Fig. 12** Electrical spectrum of a beat signal between a pilot signal and an LO under PLL operation after a 160 km transmission.

coincides with that of the LO. The linewidth of the spectrum was less than the 10 Hz frequency resolution of the electrical spectrum analyzer. The phase noise estimated by integrating the SSB noise power spectrum was 0.48 degree. Although the phase noise was increased due to the decrease in the SNR of the pilot tone signal after 160 km transmission, it was smaller than the tolerable phase noise for the 256 QAM format of 2.0 degree.

The BER performance for the polarization-multiplexed, 4 Gsymbol/s, 256 QAM transmission is shown in Fig. 13(a). Figures 13(b) and (c) show constellation maps for the back-to-back condition and after a 160 km transmission, respectively, at the maximum received power. Here, the maximum data length for demodulation was limited to 4096 symbols owing to the DSP memory size, which corresponds to a BER limit of up to  $3.1 \times 10^{-5}$ . So we used a 256 QAM signal with 4096 random patterns. This data length is shorter than that necessary to cover all symbol transition



(a) BER characteristics



(b) Back-to-back

(c) After 160 km transmission

Fig. 13 BER characteristics of Pol-Mux, 4 Gsymbol/s, 256 QAM transmission over 160 km (a) and constellations ( $4096 \times 4$  symbols) before and after 160 km transmission (b), (c).

of  $2^{16}$  ( $= 256 \times 256$ ). To confirm the pattern length independence of the demodulation performance, we evaluated the difference between the error vector magnitudes (EVM) of demodulation results obtained with our 4096 pattern data and longer data generated by using  $2^{17} - 1$  PRBS signal in a back-to-back condition. In a demodulation for the long data, multiple 4096 pattern measurements were performed and the average value of each measurement was calculated. As a result, the EVM we obtained with our 4096 pattern (1.45%) was almost the same as that obtained with the long data (1.50%). We measured the BER 10 times, and the average values are plotted in Fig. 13(a), where a broken line and two solid lines indicate a theoretical back-to-back curve and estimated BER curves for back-to-back and 160 km transmissions including the distortions caused by imperfect implementation of the hardware and the phase noise of the IF signal as shown in Fig. 12. The magnitude of the distortion produced by the hardware was calculated from the distributions of the constellations shown in Fig. 13(b). In the back-to-back condition, the estimated curve fits the experimental result well. This indicates that the difference of 2.2 dB between the theoretical and experimental values can be attributed to the incompleteness of distortion compensation for the imperfect implementation of the hardware described in Sect. 3.2. In Fig. 13(a), we plot experimental results obtained without a Raman amplifier in our previous work [15]. The power penalty after 160 km transmission was reduced from 5.3 to 2.0 dB by reducing the launch power from  $-2$

to  $-8$  dBm with a Raman amplifier. This indicates that the power penalty in our previous work was mainly caused by fiber nonlinearity such as XPM between two polarizations. The estimated BER curve does not precisely fit the experimental result obtained with the Raman amplifier. The residual 2.0 dB penalty may be caused by OSNR degradation after the 160 km transmission and residual nonlinearity. Although error free transmission was not possible, 64 Gbit/s data were transmitted over 160 km with an optical bandwidth of 5.4 GHz.

#### 4. Conclusion

We described a 160 km transmission (two 80 km spans) of a polarization-multiplexed, 4 Gsymbol/s, 256 QAM signal with an optical bandwidth of 5.4 GHz. By using a Raman amplifier and optimizing the launch power to suppress fiber nonlinearity such as XPM, the power penalty was successfully reduced from 5.3 to 2.0 dB. This result indicates the possibility of realizing an ultrahigh spectral efficiency of approximately 11 bit/s/Hz in a multi-channel transmission even when taking account of the 7% FEC overhead. Such an ultrahigh spectrally efficient transmission system would also play very important roles as regards increasing the total capacity of WDM systems and improving tolerance to chromatic dispersion and polarization mode dispersion as well as in reducing power consumption.

#### References

- [1] J. Yu, X. Zhou, M.F. Huang, Y. Shao, D. Qian, T. Wang, M. Cvijetic, P. Magill, L. Nelson, M. Birk, S. Ten, H.B. Matthew, and S.K. Mishra, "17 Tb/s ( $161 \times 114$  Gb/s) PolMux-RZ-8PSK transmission over 662 km of ultra-low-loss fiber using C-band EDFA amplification and digital coherent detection," Proc. Europ. Conf. Optical Communications, Th3.E.2, 2008.
- [2] N. Kikuchi, K. Mandai, K. Sekine, and S. Sasaki, "First experimental demonstration of single-polarization 50-Gbit/s 32-level (QASK and 8-DPSK) incoherent optical multilevel transmission," Proc. Conf. Optical Fiber Communications, PDP21, 2007.
- [3] E. Ip and J.M. Kahn, "Carrier synchronization for 3- and 4-bit-per-symbol optical transmission," J. Lightwave Technol., vol.23, pp.4110–4124, 2005.
- [4] M. Nakazawa, M. Yoshida, K. Kasai, and J. Hongou, "20 Msymbol/s, 64 and 128 QAM coherent optical transmission over 525 km using heterodyne detection with frequency-stabilized laser," Electron. Lett., vol.42, pp.710–712, 2006.
- [5] M. Nakamura, Y. Kamio, and T. Miyazaki, "Linewidth-tolerant 10-Gbit/s 16 QAM transmission using a pilot-carrier based phase-noise canceling technique," Opt. Express, vol.16, pp.10611–10616, 2007.
- [6] M. Seimetz, "Performance of coherent optical square-16-QAM-systems based on IQ-transmitters and homodyne receivers with digital phase estimation," Proc. Conf. Optical Fiber Communications, NWA4, 2006.
- [7] Y. Mori, C. Zhang, K. Igarashi, K. Katoh, and K. Kikuchi, "Phase-noise tolerance of optical 16-QAM signals demodulated with decision-directed carrier-phase estimation," Proc. Conf. Optical Fiber Communications, OWG7, 2009.
- [8] X. Zhou, J. Yu, Ting Wang, P. Magill, M. Cvijetic, L. Nelson, M. Birk, G. Zhang, Y. Yano, S. Ten, H.B. Matthew, and S.K. Mishra, "32 Tb/s ( $320 \times 114$  Gb/s) PDM-RZ-8QAM transmission

- over 580 km of ultra-low-loss fiber employing digital coherent detection and EDFA-only amplification,” Proc. Conf. Optical Fiber Communications, PDPB4, 2009.
- [9] A.H. Gnauck and P.J. Winzer, “ $10 \times 112$ -Gb/s PDM 16-QAM transmission over 1022 km of SSMF with a spectral efficiency of 4.1 b/s/Hz and no optical filtering,” Proc. Europ. Conf. Optical Communications, 8.4.2, 2009.
- [10] A.H. Gnauck, P.J. Winzer, C.R. Doerr, and L.L. Buhl, “ $10 \times 112$ -Gb/s PDM 16-QAM transmission over 630 km of fiber with 6.2-b/s/Hz spectral efficiency,” Proc. Conf. Optical Fiber Communications, PDPB8, 2009.
- [11] A. Sano, H. Masuda, T. Kobayashi, M. Fujiwara, K. Horikoshi, E. Yoshida, Y. Miyamoto, M. Matsui, M. Mizoguchi, H. Yamazaki, Y. Sakamaki, and H. Ishii, “69.1-Tb/s ( $432 \times 171$ -Gb/s) C- and extended L-band transmission over 240 km using PDM-16-QAM modulation and digital coherent detection,” Proc. Conf. Optical Fiber Communications, PDPB7, 2010.
- [12] X. Zhou, J. Yu, M.-F. Huang, Y. Shao, T. Wang, L. Nelson, P. Magill, M. Birk, P.I. Borel, D.W. Peckham, and R. Lingle, Jr., “64-Tb/s ( $640 \times 107$ -Gb/s) PDM-36QAM transmission over 320 km using both pre- and post-transmission digital equalization,” Proc. Conf. Optical Fiber Communications, PDPB9, 2010.
- [13] M. Yoshida, H. Goto, T. Omiya, K. Kasai, and M. Nakazawa, “Frequency division multiplexed 1 Gsymbol/s, 64 QAM coherent optical transmission with a spectral efficiency of 8.6 bit/s/Hz,” Proc. Europ. Conf. Optical Communications, Mo.4.D.5, 2008.
- [14] M. Nakazawa, “Challenges to FDM-QAM transmission with ultrahigh spectral efficiency,” Proc. Europ. Conf. Optical Communications, Tu.1.E.1, 2008.
- [15] M. Nakazawa, S. Okamoto, T. Omiya, K. Kasai, and M. Yoshida, “256-QAM (64 Gb/s) coherent optical transmission over 160 km with an optical bandwidth of 5.4 GHz,” IEEE Photonics Technol. Lett., vol.22, pp.185–187, 2010.
- [16] A.J. Lowery, L. Du, and J. Armstrong, “Orthogonal frequency division multiplexing for adaptive dispersion compensation in long haul WDM systems,” Proc. Conf. Optical Fiber Communications, PDP39, 2006.
- [17] Y. Ma, O. Yang, Y. Tang, S. Chen, and W. Shieh, “1-Tb/s per channel coherent optical OFDM transmission with subwavelength bandwidth access,” Proc. Conf. Optical Fiber Communications, PDPC1, 2009.
- [18] T. Omiya, H. Goto, K. Kasai, M. Yoshida, and M. Nakazawa, “24 Gbit/s, 64 QAM-OFDM coherent transmission with a bandwidth of 2.5 GHz,” Proc. Europ. Conf. Optical Communications, 1.3.2, 2009.
- [19] H. Takahashi, A.A. Amin, S.L. Jansen, I. Morita, and H. Tanaka, “ $8 \times 66.8$  Gbit/s coherent PDM-OFDM transmission over 640 km of SSMF at 5.6-bit/s/Hz spectral efficiency,” Proc. Europ. Conf. Optical Communications, Th.3.E.4, 2008.
- [20] D. Hillerkuss, T. Shellinger, R. Schmogrow, M. Winer, T. Vallaitis, R. Bonk, A. Marculescu, J. Li, M. Dreschmann, J. Meyer, S.B. Ezra, N. Narkiss, B. Nebendahl, R. Parmigiani, P. Petropoulos, B. Resan, K. Weingarten, T. Ellermeier, J. Lutz, M. Moller, M. Huebner, J. Becker, C. Koos, W. Freude, and J. Leuthold, “Signal source optical OFDM transmission and optical FFT receiver demonstrated at line rates of 5.4 and 10.8 Tbit/s,” Proc. Europ. Conf. Optical Communications, PDPC1, 2010.
- [21] H. Takahashi, A.A. Amin, S.L. Jansen, I. Morita, and H. Tanaka, “DWDM transmission with 7.0-bit/s/Hz spectral efficiency using  $8 \times 65.1$ -Gbit/s coherent PDM-OFDM signals,” Proc. Conf. Optical Fiber Communications, PDPB7, 2009.
- [22] C.E. Shannon, “A mathematical theory of communication,” Bell Syst. Tech. J., vol.27, pp.379–423 and pp.623–656, 1948.
- [23] T. Mizuochi, “Recent progress in forward error correction for optical communication systems,” IEICE Trans. Commun., vol.E88-B, no.5, pp.1934–1946, May 2005.
- [24] K. Kasai, A. Suzuki, M. Yoshida, and M. Nakazawa, “Performance improvement of an acetylene ( $C_2H_2$ ) frequency-stabilized fiber laser,” IEICE Electronics Express, vol.3, pp.487–492, no.22, 2006.
- [25] S. Shimotsu, S. Oikawa, T. Saitou, N. Mitsugi, K. Kubodera, T. Kawanishi, and M. Izutsu, “Single side-band modulation performance of a  $LiNbO_3$  integrated modulator consisting of four-phase modulator waveguides,” IEEE Photonics Technol. Lett., vol.13, pp.364–366, 2001.
- [26] K. Kasai, J. Hongo, M. Yoshida, and M. Nakazawa, “Optical phase-locked loop for coherent transmission over 500 km using heterodyne detection with fiber lasers,” IEICE Electronics Express, vol.4, no.3, pp.77–81, 2007.
- [27] A. Onae, K. Okumura, K. Sugiyama, F.L. Hong, H. Matsumoto, K. Nakazawa, R. Felder, and O. Acef, “Optical frequency standard at  $1.5 \mu m$  based on Doppler-free acetylene absorption,” Proc. 6th Symposium on Frequency Standards and Metrology, p.445, 2002.
- [28] A. Suzuki, Y. Takahashi, and M. Nakazawa, “A polarization-maintained, ultranarrow FBG filter with a linewidth of 1.3 GHz,” IEICE Electronics Express, vol.3, no.22, pp.469–473, 2006.
- [29] T. Okoshi, K. Kikuchi, and A. Nakayama, “Novel method for high resolution measurement of laser output spectrum,” Electron. Lett., vol.16, pp.630–631, 1980.
- [30] D.W. Allan, “Statistics of atomic frequency standards,” Proc. IEEE, vol.54, pp.221–230, 1966.
- [31] K. Kikuchi, T. Okoshi, M. Nagamatsu, and N. Henmi, “Degradation of bit-error rate in coherent optical communication due to spectral spread of the transmitter and the local oscillator,” J. Lightwave Technol., vol.LT-2, no.6, pp.1024–1033, 1984.
- [32] R.L. Jungerman and C.A. Flory, “Low-frequency acoustic anomalies in lithium niobate Mach-Zehnder interferometers,” Appl. Phys. Lett., vol.53, pp.1477–1479, 1988.
- [33] H. Nyquist, “Certain topics in telegraph transmission theory,” AIEE Trans., vol.47, pp.617–644, 1928.
- [34] G. Charlet, N. Maaref, J. Renaudier, H. Mardoyan, P. Tran, and S. Bigo, “Transmission of 40 Gb/s QPSK with coherent detection over ultra long haul distance improved by nonlinearity mitigation,” Proc. Europ. Conf. Optical Communications, Th4.3.4, 2006.
- [35] A. Antoniou, Digital signal processing, McGraw-Hill, New York, 2005.
- [36] J.G. Proakis, Digital Communications, 4th ed., McGraw Hill, New York, 2000.



**Masato Yoshida** received a Ph.D. degree in Electrical and Communication Engineering from Tohoku University, Miyagi, Japan, in 2001. He is currently with the Research Institute of Electrical Communication, Tohoku University. His research interests include mode-locked fiber lasers, photonic crystal fibers, and coherent optical communication. He is member of Optical Society of America (OSA), Japan Society of Applied Physics, and Laser Society of Japan.



**Seiji Okamoto** received a B.S. degree in Electrical Engineering from Tohoku University, Miyagi, Japan, in 2009. Currently he is studying toward his M.S. degree at the Research Institute of Electrical Communication, Tohoku University. His research interests include coherent optical communication.



**Tatsunori Omiya** received an M.S. degree in Electrical and Communication Engineering from Tohoku University, Miyagi, Japan, in 2009. Currently he is studying for his doctorate at the Research Institute of Electrical Communication, Tohoku University. His research interests include coherent optical communication.



**Keisuke Kasai** received a Ph.D. degree in Electrical and Communication Engineering from Tohoku University, Miyagi, Japan, in 2008. He is a research fellow of the Japan Society for the Promotion of Science (JSPS), and is currently working at the Research Institute of Electrical Communication, Tohoku University. His research interests include frequency-stabilized lasers and coherent optical communication. He is member of IEEE, Japan Society of Applied Physics, and Laser Society of Japan.



**Masataka Nakazawa** received a Ph.D. degree from the Tokyo Institute of Technology, Tokyo, Japan, in 1980. In 1980, he joined the Ibaraki Electrical Communication Laboratory, Nippon Telegraph & Telephone Public Corporation. He was a visiting scientist at Massachusetts Institute of Technology from 1984–1985. He became the first NTT R&D Fellow in 1999. In 2001, he moved to the Research Institute of Electrical Communication, Tohoku University as a professor, where he has been engaged in research on ultrahigh-speed optical communication including soliton transmission, coherent optical communication, nonlinear effects in fibers, mode-locked lasers, and photonic crystal fibers. He is now a director of the institute and a distinguished professor. He is the author and coauthor of over 400 journal articles. He holds more than 100 patents. He is a Fellow of IEEE, OSA, Japan Society of Applied Physics and has received various awards including the 2006 Thomson Scientific Laureate and the 2010 IEEE Photonics Society Quantum Electronics Award.